29th International Conference
ENGINEERING MECHANICS 2023
Milovy, Czech Republic, May 9 – 11, 2023

MECHANICAL CONCEPT OF AEROELASTIC DEMONSTRATOR AND METHODOLOGY FOR EXPERIMENTAL INVESTIGATION OF PROPELLER AERODYNAMIC DERIVATIVES

Čečrdle J.*

Abstract: *Whirl flutter is a specific type of flutter instability, for which the experimental validation of the analytical results is required. One of the key issues is the solution of propeller aerodynamic forces on a vibrating propeller. To determine propeller forces and moments, aerodynamic derivatives are used. The complete solution includes six independent derivatives, four of which may be investigated experimentally. The subjected demonstrator represents a sting-mounted nacelle with a motor and propeller. It includes engine pitch and yaw degrees-of-freedom. Both stiffness constants are adjustable and both pivots are movable in the direction of the propeller axis. For the measurement, a single degree-of-freedom model is to be used; therefore, the blocking of either pitch or yaw movement is provided. Pitching moment ($c_{m\Theta}$) and vertical force ($c_{z\Theta}$) due to the pitch angle derivatives will be measured using pitch-only model arrangement. Pitching moment ($c_{m\Psi}$) and vertical force ($c_{z\Psi}$) due to the yaw angle derivatives will be measured using yaw-only model arrangement. Measurement includes pitch and yaw angles and pitch or yaw pivot moment, respectively. To separate the contributions of both force and moment to the total moment, the measurement of two configurations varying the distance between the gimbal axis and the propeller plane is used.*

Keywords: Whirl Flutter, Propeller Aerodynamic Derivative, Aeroelastic Experiment, W-STING Demonstrator.

1. Introduction

Whirl flutter is a specific kind of aeroelastic flutter instability, which may appear on turboprop aircraft owing to the effect of rotating parts. Whirl flutter instability is driven by motion-induced unsteady aerodynamic propeller forces and moments acting in the propeller plane. It may cause unstable vibration, which can lead to a failure of an engine installation or a whole wing.

The complicated physical principle of the whirl flutter requires the experimental validation of the analytically gained results, especially due to the unreliable analytical solution of the propeller aerodynamic forces. Therefore, the aeroelastic models are used. This paper takes up the previous work on the subject by the author (Čečrdle, 2023) and describes the new demonstrator appointed to experimental investigation of a propeller aerodynamic derivatives and the methodology of the measurement.

2. Theoretical Background

The principle of whirl flutter phenomenon is described on the simple mechanical system with two degrees-of-freedom, where an engine flexible mounting is represented by two rotational springs (stiffness K_Ψ, K_Θ), while a propeller is considered rigid (see figure 1). This system has two independent mode shapes (yaw and pitch) with angular frequencies ω_Ψ and ω_Θ. Considering a propeller rotation with the angular velocity Ω, the gyroscopic effect causes both independent mode shapes merge into the whirl motion. A propeller axis shows an elliptical movement with a trajectory dependent on both angular frequencies ω_Ψ and ω_Θ. The orientation of the gyroscopic movement is backward relative to the propeller

* Ing. Jiří Čečrdle, Ph.D.: Czech Aerospace Research Centre (VZLU), Beranových 130; 199 05, Prague; CZ, cecrdle@vzlu.cz

ISSN: 1805-8256, doi: 10.21495/em2023-55

rotation for the mode with the lower frequency (backward whirl mode) and forward relative to the propeller rotation for the mode with the higher frequency (forward whirl mode).

The gyroscopic motion results in changes of the propeller blades' angles of attack. It causes generating of unsteady aerodynamic forces, which may under specific conditions induce whirl flutter instability. The critical flutter state is defined as the neutral stability with no damping of the system and the corresponding air velocity ($V = V_{FL}$) is called critical flutter speed. If the air velocity is lower than flutter speed ($V < V_{FL}$), the system is stable, and the gyroscopic motion is damped. If the airspeed exceeds the flutter speed ($V > V_{FL}$), the system becomes unstable and gyroscopic motion divergent.

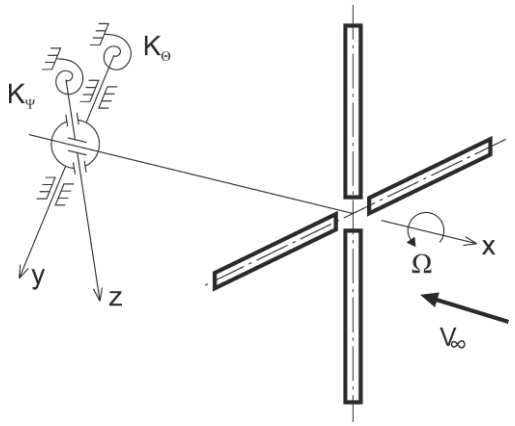

Fig. 1: Gyroscopic system with propeller

The analytical solution is focused on a determination of the aerodynamic forces caused by the gyroscopic motion on each of propeller blades. Presented equations of motion were derived for the gyroscopic system shown in figure 1 using Lagrange's approach. Three angles (φ, Θ, Ψ) are independent generalized coordinates, the propeller angular velocity is constant ($\varphi = \Omega\, t$). The rotating part is assumed cyclically symmetric with respect to both mass and aerodynamics. Non-uniform mass moments of inertia of an engine with respect to pitch and yaw axes ($J_Z \neq J_Y$) are considered. Considering small angles, the equations of motion become:

$$J_Y\ddot{\Theta} + \left(K_\Theta\gamma_\Theta/\omega\right)\dot{\Theta} + J_X\Omega\dot{\Psi} + K_\Theta\Theta = M_{YP} - aP_Z$$
$$J_Z\ddot{\Psi} + \left(K_\Psi\gamma_\Psi/\omega\right)\dot{\Psi} + J_X\Omega\dot{\Theta} + K_\Psi\Psi = M_{ZP} + aP_Y \qquad (1)$$

Propeller aerodynamic forces (right-hand side of eqn. 1, see also figure 2) are determined using aerodynamic derivatives (Ribner, 1945; Houbolt and Reed, 1962). Neglecting the aerodynamic inertia terms, the equations for the propeller's dimensionless forces and moments may be expressed as follows:

$$P_Y = qS\left(c_{y\Psi}\Psi^* + c_{y\Theta}\Theta^* + c_{y\mathrm{q}}\left(\dot{\Theta}^* D/2V\right)\right) \qquad P_Z = qS\left(c_{z\Psi}\Psi^* + c_{z\Theta}\Theta^* + c_{z\mathrm{r}}\left(\dot{\Psi}^* D/2V\right)\right)$$
$$M_{YP} = qSD\left(c_{m\Psi}\Psi^* + c_{m\mathrm{q}}\left(\dot{\Theta}^* D/2V\right)\right) \qquad M_{ZP} = qSD\left(c_{n\Theta}\Theta^* + c_{n\mathrm{r}}\left(\dot{\Psi}^* D/2V\right)\right) \qquad (2)$$

Where q is a dynamic pressure, S is a propeller disc area, D is a propeller diameter, Θ* and Ψ* are effective pitch and yaw angles, respectively. The aerodynamic derivatives (c-terms) are defined as follows:

$$c_{y\Theta} = \partial c_y/\partial\Theta^* \quad c_{y\Psi} = \partial c_y/\partial\Psi^* \quad c_{y\mathrm{q}} = \partial c_y/\partial\left(\dot{\Theta}D/2V\right) \quad c_{y\mathrm{r}} = \partial c_y/\partial\left(\dot{\Psi}D/2V\right)$$
$$c_{z\Theta} = \partial c_z/\partial\Theta^* \quad c_{z\Psi} = \partial c_z/\partial\Psi^* \quad c_{z\mathrm{q}} = \partial c_z/\partial\left(\dot{\Theta}D/2V\right) \quad c_{z\mathrm{r}} = \partial c_z/\partial\left(\dot{\Psi}D/2V\right)$$
$$c_{m\Theta} = \partial c_m/\partial\Theta^* \quad c_{m\Psi} = \partial c_m/\partial\Psi^* \quad c_{m\mathrm{q}} = \partial c_m/\partial\left(\dot{\Theta}D/2V\right) \quad c_{m\mathrm{r}} = \partial c_m/\partial\left(\dot{\Psi}D/2V\right)$$
$$c_{n\Theta} = \partial c_n/\partial\Theta^* \quad c_{n\Psi} = \partial c_n/\partial\Psi^* \quad c_{n\mathrm{q}} = \partial c_n/\partial\left(\dot{\Theta}D/2V\right) \quad c_{n\mathrm{r}} = \partial c_n/\partial\left(\dot{\Psi}D/2V\right) \qquad (3)$$

Considering the symmetry (or antisymmetry), we can reduce the number of derivatives as follows:

$$c_{z\Psi} = c_{y\Theta};\ c_{m\Psi} = -c_{n\Theta};\ c_{m\mathrm{q}} = c_{n\mathrm{r}};\ c_{z\mathrm{r}} = c_{y\mathrm{q}};\ c_{z\Theta} = -c_{y\Psi};\ c_{n\Psi} = c_{m\Theta};\ c_{m\mathrm{r}} = -c_{n\mathrm{q}};\ c_{y\mathrm{r}} = -c_{z\mathrm{q}} \qquad (4)$$

In addition, we can neglect the negligible derivatives: $c_{m\mathrm{r}} = -c_{n\mathrm{q}} = 0$ and $c_{y\mathrm{r}} = -c_{z\mathrm{q}} = 0$. Finally, we obtain six independent derivatives: $c_{z\Theta}$, $c_{m\Theta}$, $c_{z\Psi}$, $c_{m\Psi}$, $c_{m\mathrm{q}}$ and $c_{z\mathrm{r}}$. The first four ones may be investigated experimentally.

3. Aeroelastic Demonstrator (W-STING)

Aeroelastic demonstrator for investigation of a propeller aerodynamic derivatives (W-STING) represents a sting-mounted nacelle with a motor and propeller. The demonstrator includes two degrees-of-freedom

(engine pitch and yaw). For the measurement, just a single degree-of-freedom is used and other one is mechanically blocked. The stiffness parameters in both pitch and yaw are modelled by means of cross spring pivots with changeable spring leaves. Stiffness constants are independently adjustable by replacing these spring leaves. Both pivots can be independently moved in the direction of the propeller axis within the range of 0.15 m to adjust the pivot points of both vibration modes. The demonstrator is capable of simulating changes of all the important parameters influencing the whirl flutter. The centre of the gravity of the nacelle can be adjusted by means of the movable balance weight. The plastic nacelle cowling is manufactured using the 3D print technology. The gyroscopic effect of the rotating mass is simulated by the mass of the propeller blades. Two sets of blades made of duralumin and steel are available. The propeller with *D = 0.7 m* represents a scaled-down real 5-blade propeller. The propeller blades' angle of attack is adjustable at the standstill by means of the special tool. The propeller is powered by an electric motor. The demonstrator sensor instrumentation includes measurements of both pitch and yaw angles and the measurement of both pitch and yaw pivot moments. In addition, propeller parameters (thrust, rpm, etc.) are measured as well. The system is controlled by the special in-house LabVIEW-based SW tool. The nacelle design drawing is shown in figure 3.

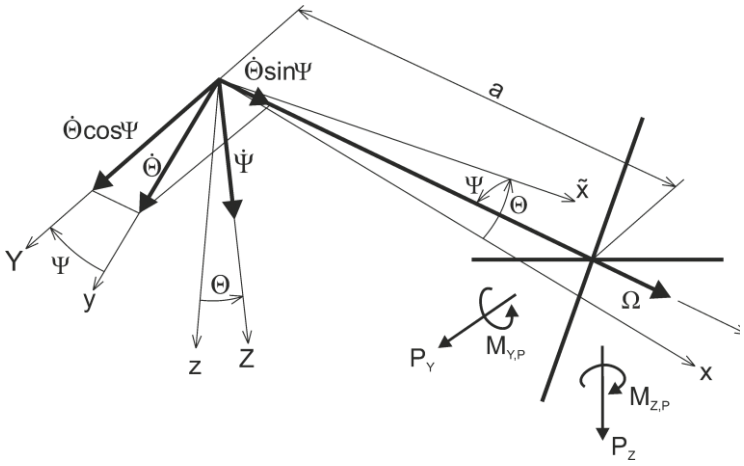

Fig. 2: Kinematical scheme of gyroscopic system, propeller plane aerodynamic forces and moments

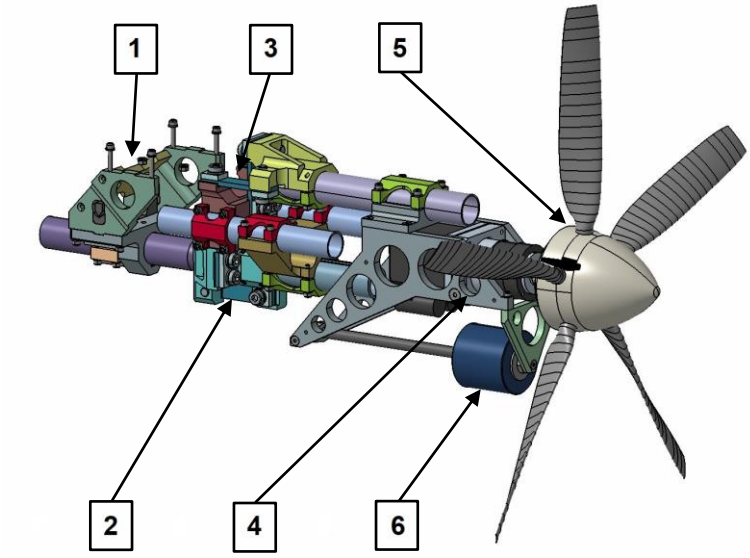

Fig. 3: W-STING demonstrator, uncoated nacelle with motor and propeller (1 – sting attachment; 2 – yaw attachment; 3 – pitch attachment; 4 – motor; 5 – propeller; 6 – massbalance weight.

4. Methodology of Measurement

The static equations for the engine and propeller pitch and yaw deflection may be (from eqn. 1) expressed using the total moment-related derivatives (denoted by *) as:

$$k^2\Theta = \kappa(c^*_{m\Theta}\Theta + c^*_{m\Psi}\Psi) \qquad k^2\Psi = \kappa(c^*_{n\Psi}\Psi + c^*_{n\Theta}\Theta) \tag{5}$$

Note that the relations $c^*_{m\Theta} = c^*_{n\Psi}$ and $c^*_{m\Psi} = -c^*_{n\Theta}$ given by eqn. 4 were used in the latter equation.

For determination of $c_{m\Theta}$ and $c_{z\Theta}$ derivatives, the pitch-only arrangement of the demonstrator is used. Hence, for $\Psi = 0$, the total pitching moment coefficient (c^*_m) may be expressed as:

$$c^*_m = (K_\Theta\Theta/qSD) \tag{6}$$

Where $K_\Theta\Theta$ is the measured pitch pivot moment. The measurement is performed varying the pitch angle (by manipulator) and the moment is evaluated with respect to the pitch angle (Θ). The slope of the measured curves is the reference pitch moment due to pitch angle derivative ($c^*_{m\Theta}$). To separate the force

and moment contributions to the total pitch moment, two configurations varying the distance between the gimbal axis and the propeller plane (***a***) are measured. The equations are:

$$c^*_{m\Theta 1} = c_{m\Theta} - (a_1/D)c_{z\Theta} \qquad c^*_{m\Theta 2} = c_{m\Theta} - (a_2/D)c_{z\Theta} \tag{7}$$

And the final expressions for aerodynamic derivatives become:

$$c_{m\Theta} = \big(1/(a_2 - a_1)\big)(a_2 c^*_{m\Theta 1} - a_1 c^*_{m\Theta 2}) \qquad c_{z\Theta} = \big(D/(a_2 - a_1)\big)(c^*_{m\Theta 1} - c^*_{m\Theta 2}) \tag{8}$$

For determination of $c_{m\Psi}$ and $c_{z\Psi}$ derivatives, the yaw-only arrangement of the demonstrator is used. Hence, the total yawing moment coefficient (c_n^{**}) may be expressed as:

$$c_n^{**} = (K_\Psi \Psi / qSD) = (c^*_{n\Psi}\Psi + c^*_{n\Theta}\Theta) \tag{9}$$

Where $K_\Psi\Psi$ is the measured yaw pivot moment. The measurement is performed varying the pitch angle (by manipulator) and the moment is evaluated with respect to this pitch angle (Θ). The slope of the measured curves ($c^{**}_{n\Theta}$) and eqn. (9) are used to obtain the reference yaw moment due to pitch angle derivative ($c^*_{n\Theta}$) that is:

$$c^*_{n\Theta} = \big(c^{**}_{n\Theta} - c^*_{n\Psi}(\Psi/\Theta)\big) \tag{10}$$

The yaw-to-pitch angle ratio (Ψ/Θ) is constant just for a given blade angle and dynamic pressure. Since the (Ψ/Θ) ratio is dynamic pressure dependent, the yawing moment coefficient (c_n^{**}) is dynamic pressure dependent as well. The reference yaw moment due to yaw angle derivative ($c^*_{n\Psi}$) is obtained using the antisymmetry (eqn. (4)) as $c^*_{n\Psi} = c^*_{m\Theta}$. Similarly, we use $c^*_{n\Theta} = -c^*_{m\Psi}$ to obtain the reference pitch moment due to yaw angle derivative ($c^*_{m\Psi}$). Separation of ($c^*_{m\Psi}$) to its components ($c_{m\Psi}$) and ($c_{z\Psi}$), i.e., the separation of force and moment contributions is carried out similarly as mentioned above, i.e., by measuring of two configurations varying the distance between the gimbal axis and the propeller plane (a). The final expressions for aerodynamic derivatives are:

$$c_{m\Psi} = \big(1/(a_2 - a_1)\big)(a_1 c^*_{n\Theta 2} - a_2 c^*_{n\Theta 1}) \qquad c_{z\Psi} = \big(D/(a_2 - a_1)\big)(c^*_{n\Theta 2} - c^*_{n\Theta 1}) \tag{11}$$

5. Conclusion and Outlook

The paper deals with the mechanical concept of the aeroelastic demonstrator for the measurement of a propeller aerodynamic derivatives (W-STING). The demonstrator represents a sting-mounted nacelle with the engine and thrusting propeller. The demonstrator's concept allows adjusting of all main parameters influencing whirl flutter. A broad testing campaign in the VZLU 3m-diameter wind tunnel is planned. The test schedule includes the measurement of four aerodynamic derivatives. Secondary variable parameters include the airflow velocity (dynamic pressure) and a blade angle of attack. The experimental results will be subsequently utilised for verification of the analytical models and computational tools (Dugeai et. al., 2011, Sicot and Dugeai, 2011) that will be used for development of the new power plant system, characterised as an open-fan concept, utilised for a new generation short-medium range turboprop aircraft.

Acknowledgement

Program and topic: HORIZON-JU-CLEAN-AVIATION-2022-01-SMR-01, Ultra Efficient Propulsion Systems for Short and Short-Medium Range Aircraft. Project nr. and title: 101102011, Open Fan for Environmental Low Impact of Aviation (OFELIA).

References

Čečrdle, J. (2023) Whirl Flutter of Turboprop Aircraft Structures, 2nd Ed., Elsevier Science.

Houbolt, J.C. and Reed, W.H. (1962) Propeller Nacelle Whirl Flutter, Journal of Aerospace Sciences, 29:333-346, Mar 1962.

Ribner, H.S. (1945) Propellers in Yaw, NACA Report 820.

Dugeai, A., Mauffrey, Y. and Sicot, F. (2011) Aeroelastic Capabilities of the elsA Solver for Rotating Machines Applications, in: Proc. Int. Forum on Aeroelasticity and Structural Dynamics, Paris, France.

Sicot, F. and Dugeai, A. (2011) Numerical Investigation of Propellers Whirl Flutter Using elsA, in: Proc. Int. Forum on Aeroelasticity and Structural Dynamics, Paris, France.